ChemComm

COMMUNICATION

View Article Online
View Journal | View Issue

Published on 29 October 2014. Downloaded by Dalian Institute of Chemical Physics, CAS on 4/29/2020 9:12:02 AM.

Cite this: *Chem. Commun.*, 2014, 50, 15811

Received 10th October 2014,
Accepted 23rd October 2014

DOI: 10.1039/c4cc08010f

www.rsc.org/chemcomm

A twisted-intramolecular-charge-transfer (TICT) based ratiometric fluorescent thermometer with a mega-Stokes shift and a positive temperature coefficient†

Cheng Cao,[ab] Xiaogang Liu,*[bc] Qinglong Qiao,[b] Miao Zhao,[b] Wenting Yin,[b] Deqi Mao,[b] Hui Zhang*[a] and Zhaochao Xu*[b]

The fluorescence intensity of *N,N*-dimethyl-4-((2-methylquinolin-6-yl)ethynyl)aniline exhibits an unusual intensification with increasing temperature, by activating more vibrational bands and leading to stronger TICT emissions upon heating in dimethyl sulfoxide. Based on the different temperature dependence at various wavelengths, as shown in the TICT fluorescence spectrum, this dye can be employed to ratiometrically detect temperature.

Fluorescent thermometers have been actively investigated for visualizing temperature distribution in micro-environments with high spatial and temporal resolutions, *i.e.*, in cells and micro-fluidic devices.[1–8] Most of such thermometers are based on temperature-sensitive organic dyes (such as rhodamine B) or inorganic complexes of ruthenium or europium, whilst their emission intensities/lifetimes decrease with rising temperature (owing to the thermal activation of nonradiative de-excitation pathways), and this correlation affords temperature information.[9–13] Recently, CdSe quantum dots[14] and ZnO microcrystals[15] have also been reported as nano-thermometers, which, however, still possess a negative temperature coefficient. In contrast, fluorescent probes with a positive temperature coefficient, whose emission intensities increase with temperature, are particularly desirable, because they can effectively suppress background interference at high temperature; they can also work in conjunction with one fluorophore with a negative temperature coefficient, where ratiometric measurements of their emission intensities provide a built-in correction and allow quantitative detection of temperature with high sensitivity.[2,16–19] To this end, a number of polymer-based fluorescent thermometers, which consist of a thermo-responsive polymer and a polarity-sensitive fluorophore fragment (such as benzofurazan), have been reported to have positive temperature coefficients,[20–22] because polymers offer a decreasing micro-environmental polarity around the fluorophore with a rise in temperature. Unfortunately, these polymer-based thermometers require complicated synthesis procedures; their temperature sensing functionality only operates around the polymer phase transition point (where significant micro-polarity changes occur) and the corresponding working range is thus limited (*i.e.*, <10 °C). A fluorophore with a positive temperature coefficient has also been reported based on the thermally activated delayed fluorescence of fullerene C_{70}, whilst an increase in temperature facilitates the back–forth transitions between the excited states S_1 (singlet) and T_1 (triplet).[23] Nevertheless, such an effect is vulnerable to oxygen quenching, posing a significant limitation to its application environment. Consequently, the development of new fluorescent thermometers, preferably with positive temperature coefficients, ratiometric measurements and a wide working range becomes an important research target.

In this work, we propose and demonstrate a new design concept to achieve a positive temperature coefficient in a fluorescent thermometer, employing the twisted-intramolecular-charge-transfer (TICT) emission of *N,N*-dimethyl-4-((2-methylquinolin-6-yl)ethynyl)aniline (**1**; Scheme 1) in dimethyl sulfoxide (DMSO). TICT emission is typically weak, because emission from the zero vibrational level of the TICT state is forbidden; in contrast, the radiative transitions from TICT to ground states are feasible *via* the assistance of higher

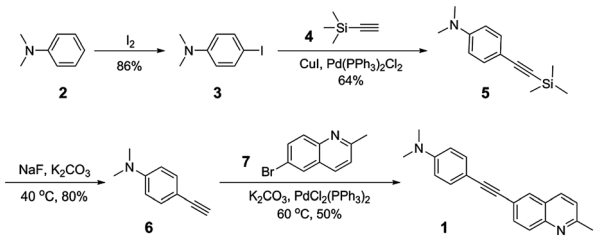

Scheme 1 The synthesis route of **1**.

[a] *School of Pharmaceutical Engineering, Shenyang Pharmaceutical University, Shenyang 110016, China. E-mail: zh19683@163.com*
[b] *Key Laboratory of Separation Science for Analytical Chemistry, Dalian Institute of Chemical Physics, Chinese Academy of Sciences, Dalian 116023, China. E-mail: zcxu@dicp.ac.cn*
[c] *Singapore-MIT Alliance for Research and Technology (SMART) Centre, 1 CREATE Way, Singapore 138602, Singapore. E-mail: xgliu83@gmail.com*

† Electronic supplementary information (ESI) available: Synthesis, characterization, experimental and computational details. See DOI: 10.1039/c4cc08010f

Published on 29 October 2014. Downloaded by Dalian Institute of Chemical Physics, CAS on 4/29/2020 9:12:02 AM.

and non-totally symmetrical vibrational bands of the TICT state.[24] These vibrational bands become activated upon heating. Consequently, the TICT emission intensity will become intensified with increasing temperature, provided that the increase in the TICT emission rate exceeds that of non-emissive de-excitation.

Compound **1** was synthesized in good yield, as shown in Scheme 1 (ESI,† Fig. S1–S3). The UV-vis absorption solvatochromism of **1** is very weak (Fig. 1a). For example, the peak UV-vis absorption wavelength (λ_{abs}) of **1** changes from 332 nm in *n*-hexane to 338 nm in DMSO, by only 6 nm. In contrast, the peak emission wavelength (λ_{em}) of **1** in solution varies considerably from non-polar to polar solvents (Fig. 1b). For instance, the peak λ_{em} is registered at 380 nm in *n*-hexane and ~550 nm in DMSO, with a change of ~170 nm. The substantial bathochromic shift in the peak λ_{em} results in a mega-Stokes shift of ~210 nm in DMSO. A mega-Stokes shift is beneficial for reducing the overlap between the UV-vis absorption and emission spectra of a fluorophore and for minimizing the re-absorption of the emitted photons (*via* the so called "inner-filter" effect), and thus improves the signal-to-noise ratio of fluorescence imaging.[25]

It is worth noting that the emission spectrum of **1** in *n*-hexane exhibits a clear shoulder; however, the fluorescence spectra become featureless with large Stokes shifts, as solvent polarity increases (Fig. 1b). Moreover, the transition energy of the fluorescence (ν_{em}) and Δf, the orientation polarisability (eqn (1)), demonstrate an approximate linear relationship in most solvents, except in *n*-hexane, as shown in a Lippert–Mataga plot (correlation coefficient, r = 0.9287; Fig. 1c; Table S1, ESI†). Interestingly, by re-plotting ν_{em} against $\Delta f'$ (eqn (2); which is applicable when the TICT state is formed upon photoexcitation of a dye), an even higher correlation coefficient of 0.9507 is obtained (excluding data in *n*-hexane; Fig. S4, ESI†).[26] These unusual spectral characteristics indicate the formation of the TICT state in the excited state of **1**.

$$\Delta f = \frac{\varepsilon - 1}{2\varepsilon + 1} - \frac{n^2 - 1}{2n^2 + 1} \quad (1)$$

$$\Delta f' = \frac{\varepsilon - 1}{\varepsilon + 2} - \frac{n^2 - 1}{2n^2 + 4} \quad (2)$$

where ε and n refer to the relative dielectric constant and the refractive index of a solvent, respectively.

The formation of the TICT state in **1** can be further rationalised *via* both viscosity-dependent emission measurements and density functional theory (DFT) based calculations. In the mixtures of ethanol and glycerol at various ratios, the UV-vis absorption spectra of **1** remain little changed (Fig. 2a). In contrast, as more glycerol is added into the mixture, affording a higher viscosity, the corresponding emission intensity of **1** is significantly enhanced, *i.e.*, approximately three times from pure ethanol to pure glycerol (Fig. 2b). Such viscosity-dependent fluorescence intensification is a typical characteristic of TICT emission.[24,27] Furthermore, DFT calculations show that the photoexcitation of **1** from S_0 to S_1 states mainly involves electron transitions from the highest occupied molecular orbital (HOMO) to both the lowest occupied molecular orbital (LUMO) and LUMO + 1 (Fig. 2c). Such transitions result in substantial intramolecular charge transfer (ICT) from the phenyl ring to the quinolone ring of **1**. A large extent of ICT is accompanied by significant molecular geometry relaxation and drives the formation of the TICT state at the excited state of **1**, *via* the rotation of the dimethyl-amino group. The substantial geometry relaxation in conjunction with the greatly increased

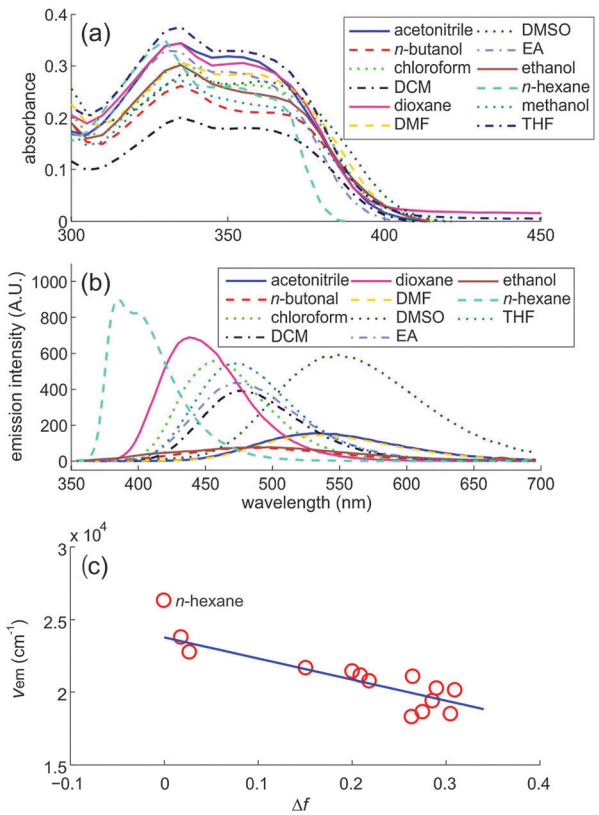

Fig. 1 (a) The UV-vis absorption and (b) fluorescence spectra of **1** in various solvents. (c) The Lippert–Mataga plot for the fluorescence transition energies of **1**. [**1**] = 10 μM; the fluorescence spectra were obtained by exciting the samples at their respective peak UV-vis absorption wavelengths. Note that the scales in (b) are arbitrary, owing to varied slit sizes in use; please refer to Table S1 (ESI†) for exact fluorescence quantum yields in various solvents.

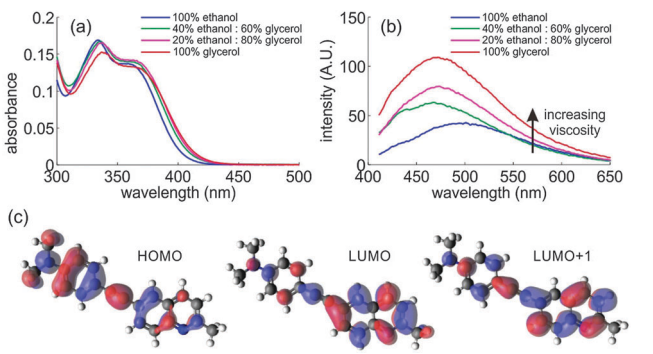

Fig. 2 (a) The UV-vis absorption and (b) fluorescence spectra of **1** in ethanol–glycerol mixtures. [**1**] = 5 μM; the fluorescence spectra were obtained by exciting the samples at 380 nm. (c) The frontier molecular orbitals of **1** in DMSO, obtained *via* DFT calculations.

 This journal is © The Royal Society of Chemistry 2014

Published on 29 October 2014. Downloaded by Dalian Institute of Chemical Physics, CAS on 4/29/2020 9:12:02 AM.

polarity of **1** in the TICT state is responsible for the mega-Stokes shift of **1** and its large fluorescence solvatochromism.[25,28]

The emission intensities of **1** between ~450 and ~600 nm exhibit an unusual positive temperature coefficient, with a temperature coefficient of 0.5% per °C, while that in the long-wavelength region (>600 nm) decreases slightly with increasing temperature in DMSO (Fig. 3a). Accordingly, the fluorescence quantum yield of **1** increases as temperature rises in DMSO (Table S2, ESI†). This extraordinary effect can be rationalised considering the nature of TICT emissions. As temperature rises, more vibrational bands at higher energy levels in the TICT state become active, which boosts the probability of radiative electron transitions from TICT to ground states. Not surprisingly, the associated peak emission wavelength of **1** also displays a blue-shift from 551 nm at 25 °C to 538 nm at 65 °C, because TICT emissions associated with higher vibrational bands contribute relatively more as temperature increases (Fig. 3a).[24]

It should be pointed out that the overall temperature dependence of fluorescence intensity depends on two competing factors, the rates of radiative TICT emission and non-emissive de-excitation. Both rates increase with rising temperature. While the former is relatively more significant, such as in DMSO, **1** demonstrates a positive temperature coefficient (Fig. 3a); in contrast, an inverse trend is found in other solvents, such as ethyl acetate (EA; Fig. 3b), owing to more substantial non-emissive de-excitation at high temperature. Consequently, the emission quantum yield of 1 drops with increasing temperature (Table S2, ESI†). In fact, the fluorescence intensities of most TICT dyes decrease at high temperature.[11]

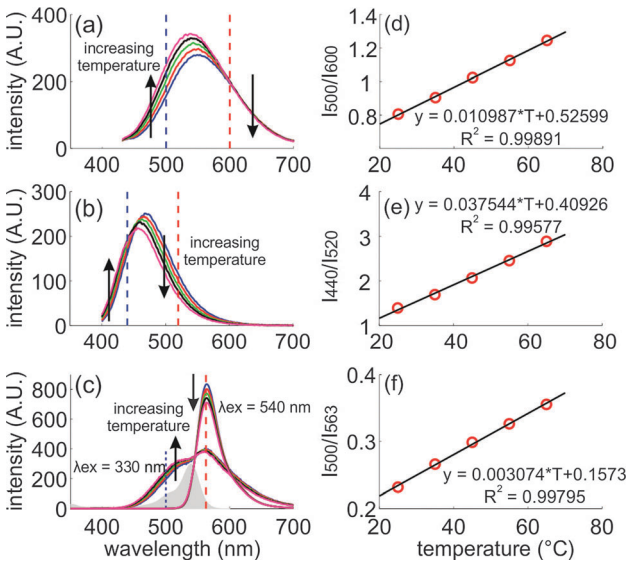

Fig. 3 Temperature dependence of the fluorescence spectra of (a) **1** in DMSO excited at 360 nm ([**1**] = 5 μM); (b) **1** in EA excited at 360 nm ([**1**] = 1 μM); (c) the mixture of **1** and rhodamine 6G in DMSO excited at 330 and 540 nm, respectively; [**1**] = 5 μM; [rhodamine 6G] = 1 μM. Temperature was varied from 25 to 65 °C at a step change of 10 °C. The corresponding temperature dependence of emission intensity ratios and the associated best-fit equations of (d) **1** in DMSO at 500 and 600 nm; (e) **1** in EA at 440 and 520 nm; (f) **1** and the rhodamine 6G mixture in DMSO at 500 and 563 nm.

The different temperature dependence of TICT emissions at varied wavelengths can be employed for ratiometric temperature measurements (Fig. 3). The ratios of emission intensities at 500 and 600 nm in DMSO ([**1**] = 5 μM; λ_{ex} = 360 nm) afford an excellent linear correlation with temperature changes, which demonstrates the potential of using **1** as a thermometer (Fig. 3d). A similar temperature calibration curve has also been constructed in other solvents, *i.e.*, EA, although the overall emission intensity of **1** drops as temperature increases in this case (Fig. 3e). The reversibility of this fluorescent system was also investigated by heating and cooling it between 25 °C and 65 °C at a step change of 10 °C for 10 cycles in DMSO. The fluorescence intensities at different temperatures remain consistent among all cycles, demonstrating an excellent reversibility.

Compound **1** can also work in conjunction with a temperature sensitive fluorophore, *i.e.*, rhodamine 6G with a negative temperature coefficient, to ratiometrically detect temperature in DMSO (Fig. 3c and f). It is interesting to note that Förster resonance energy transfer (FRET) from **1** to rhodamine 6G occurs in this mixture, because the UV-vis absorption spectrum of rhodamine 6G (represented by the grey shadowed area in Fig. 3c) matches the emission spectrum of **1** very well. As a result, an emission peak at 567 nm, owing to rhodamine 6G, became apparent even when the mixture was excited at 330 nm.

The TICT based thermometer of **1** circumvents several limitations of existing fluorescent temperature sensors. Fluorescence lifetime-based thermometers require relatively long measurement times and sophisticated equipment.[11] Fluorescence intensity-based measurements are more straightforward. However, the emission intensity also depends on the dye concentration and the illumination intensity. Careful initial calibration is thus unavoidable when a single type of dye is employed in a thermometer. While a ratiometric thermometer using two types of dyes with distinct temperature coefficients provides a built-in correction, these two types of dyes may photo-bleach at different rates, thus compromising the reliability of the thermometer.[4] Moreover, the inhomogeneous distribution of dyes (or concentration ratios) in a complex system is a major concern for accurate interpretations of emission intensity signals for both one-dye and two-dye thermometers. In contrast, the thermometer based on **1** offers a ratiometric temperature sensing mechanism, while only one type of dye is employed. This self-calibration effect makes the thermometer insensitive to dye concentration variations and photo-bleaching effects, thus greatly improving measurement accuracy. In addition, although the emission brightness of TICT dyes is normally low, the quantum yields of **1** are good, measured to be 55.2% and 18.9% at 25 °C in EA and DMSO, respectively (Table S2, ESI†). Since the temperature calibration curve of **1** is solvent-dependent and viscosity-dependent, this thermometer is most suitable for a system with minimal solvent and viscosity variations. It can also serve as a calibration reference for existing one-dye and two-dye thermometers to further gauge their accuracies, *i.e.*, in cells where the environment mostly consists of water.

In conclusion, we have demonstrated a TICT induced emission system with a positive temperature coefficient and a mega-Stokes shift based on **1**. This unusual positive temperature coefficient is

Published on 29 October 2014. Downloaded by Dalian Institute of Chemical Physics, CAS on 4/29/2020 9:12:02 AM.

realised by significantly activating vibrational bands of the TICT state, which greatly facilitates TICT emissions with respect to non-emissive de-excitation with a rise in temperature. Owing to different temperature dependence of TICT fluorescence at various wavelengths, the intensity ratios of these emissions can be used to ratiometrically detect temperature. It is expected that this new sensor design strategy will have a significant impact on the development of ratiometric fluorescent thermometers. However, **1** has poor solubility in aqueous solution and relatively short absorption wavelengths. Developing water-soluble and bathochromically shifted TICT dyes is the subject of our future work, for measuring temperature in biological systems. The molecular origins of the unusually high quantum yields and positive temperature coefficients associated with the TICT emission of **1** are also currently under investigation.

Z.X. is grateful for the financial support from the National Natural Science Foundation of China (21276251 and 21422606), the Ministry of Human Resources and Social Security of PRC, the 100 talents program funded by Chinese Academy of Sciences. X.L. thanks the National Research Foundation of Singapore for the SMART Scholar Postdoctoral Scholarship.

Notes and references

1 C. Gosse, C. Bergaud and P. Low, in *Thermal Nanosystems and Nanomaterials*, ed. S. Volz, 2009, vol. 118, pp. 301–341.
2 E. J. McLaurin, L. R. Bradshaw and D. R. Gamelin, *Chem. Mater.*, 2013, **25**, 1283–1292.
3 T. Ozawa, H. Yoshimura and S. B. Kim, *Anal. Chem.*, 2013, **85**, 590–609.
4 X. D. Wang, O. S. Wolfbeis and R. J. Meier, *Chem. Soc. Rev.*, 2013, **42**, 7834–7869.
5 Z. Yang, J. Cao, Y. He, J. H. Yang, T. Kim, X. Peng and J. S. Kim, *Chem. Soc. Rev.*, 2014, **43**, 4563–4601.
6 K. Okabe, N. Inada, C. Gota, Y. Harada, T. Funatsu and S. Uchiyama, *Nat. Commun.*, 2012, **3**, 705.
7 S. Kiyonaka, T. Kajimoto, R. Sakaguchi, D. Shinmi, M. Omatsu-Kanbe, H. Matsuura, H. Imamura, T. Yoshizaki, I. Hamachi, T. Morii and Y. Mori, *Nat. Methods*, 2013, **10**, 1232–1238.
8 T. J. Johnson, D. Ross and L. E. Locascio, *Anal. Chem.*, 2001, **74**, 45–51.
9 N. Chandrasekharan and L. A. Kelly, *J. Am. Chem. Soc.*, 2001, **123**, 9898–9899.
10 S. Ryu, I. Yoo, S. Song, B. Yoon and J. M. Kim, *J. Am. Chem. Soc.*, 2009, **131**, 3800–3801.
11 J. Feng, K. Tian, D. Hu, S. Wang, S. Li, Y. Zeng, Y. Li and G. Yang, *Angew. Chem., Int. Ed.*, 2011, **50**, 8072–8076.
12 Y. Jiang, X. Yang, C. Ma, C. Wang, Y. Chen, F. Dong, B. Yang, K. Yu and Q. Lin, *ACS Appl. Mater. Interfaces*, 2014, **6**, 4650–4657.
13 V. F. Pais, J. M. Lassaletta, R. Fernandez, H. S. El-Sheshtawy, A. Ros and U. Pischel, *Chemistry*, 2014, **20**, 7638–7645.
14 L. M. Maestro, E. M. Rodriguez, F. S. Rodriguez, M. C. la Cruz, A. Juarranz, R. Naccache, F. Vetrone, D. Jaque, J. A. Capobianco and J. G. Sole, *Nano Lett.*, 2010, **10**, 5109–5115.
15 S. L. Shinde and K. K. Nanda, *Angew. Chem., Int. Ed.*, 2013, **52**, 11325–11328.
16 Y. Takei, S. Arai, A. Murata, M. Takabayashi, K. Oyama, S. Ishiwata, S. Takeoka and M. Suzuki, *ACS Nano*, 2014, **8**, 198–206.
17 T. Kan, H. Aoki, N. Binh-Khiem, K. Matsumoto and I. Shimoyama, *Sensors*, 2013, **13**, 4138–4145.
18 A. E. Albers, E. M. Chan, P. M. McBride, C. M. Ajo-Franklin, B. E. Cohen and B. A. Helms, *J. Am. Chem. Soc.*, 2012, **134**, 9565–9568.
19 F. Ye, C. Wu, Y. Jin, Y. H. Chan, X. Zhang and D. T. Chiu, *J. Am. Chem. Soc.*, 2011, **133**, 8146–8149.
20 C. Gota, K. Okabe, T. Funatsu, Y. Harada and S. Uchiyama, *J. Am. Chem. Soc.*, 2009, **131**, 2766–2767.
21 S. Uchiyama, Y. Matsumura, A. P. de Silva and K. Iwai, *Anal. Chem.*, 2004, **76**, 1793–1798.
22 S. Uchiyama, N. Kawai, A. P. de Silva and K. Iwai, *J. Am. Chem. Soc.*, 2004, **126**, 3032–3033.
23 C. Baleizão, S. Nagl, S. M. Borisov, M. Schäferling, O. S. Wolfbeis and M. N. Berberan-Santos, *Chem. – Eur. J.*, 2007, **13**, 3643–3651.
24 Z. R. Grabowski, K. Rotkiewicz and W. Rettig, *Chem. Rev.*, 2003, **103**, 3899–4032.
25 X. Liu, Z. Xu and J. M. Cole, *J. Phys. Chem. C*, 2013, **117**, 16584–16595.
26 B. Valeur, *Molecular Fluorescence: Principles and Applications*, John Wiley & Sons, 2013.
27 M. K. Kuimova, G. Yahioglu, J. A. Levitt and K. Suhling, *J. Am. Chem. Soc.*, 2008, **130**, 6672–6673.
28 X. Liu, J. M. Cole and K. S. Low, *J. Phys. Chem. C*, 2013, **117**, 14731–14740.

 This journal is © The Royal Society of Chemistry 2014